Phase Structure and Viscoelastic Properties of Compatibilized Blends of PET and HDPE Recyclates

MIROSŁAW PLUTA,[1] ZBIGNIEW BARTCZAK,[1] ANDRZEJ PAWLAK,[1] ANDRZEJ GALESKI,[1] MARIANO PRACELLA[2]

[1]Centre of Molecular and Macromolecular Studies, Polish Academy of Sciences, Sienkiewicza 112, 90-363 Lodz, Poland

[2]Centro Studi Materiali Macromolecolari Polifasici e Biocompatibili, CNR, Via Diotisalvi 2, 56126 Pisa, Italy

Received 10 July 2000; accepted 25 February 2001

ABSTRACT: Immiscible blends of recycled poly(ethylene terephthalate) (R-PET), containing some amount of polymeric impurities, and high-density polyethylene (R-PE), containing admixture of other polyolefins, in weight compositions of 75 : 25 and 25 : 75 were compatibilized with selected compatibilizers: maleated styrene–ethylene/butylene–styrene block copolymer (SEBS-*g*-MA) and ethylene–glycidyl methacrylate copolymer (EGMA). The efficiency of compatibilization was investigated as a function of the compatibilizer content. The rheological properties, phase structure, thermal, and viscoelastic behavior for compatibilized and binary blends were studied. The results are discussed in terms of phase morphology and interfacial adhesion among components. It was shown that the addition of the compatibilizer to R-PET-rich blends and R-PE-rich blends increases the melt viscosity of these systems above the level characteristic for the respective binary blends. The dispersion of the minor phase improved with increasing compatibilizer content, and the largest effects were observed for blends compatibilized with EGMA. Calorimetric studies indicated that the presence of a compatibilizer had a slight affect on the crystallization behavior of the blends. The dynamic mechanical analysis provided evidence that the occurrence of interactions of the compatibilizer with blend components occurs through temperature shift and intensity change of a β-relaxation process of the PET component. An analysis of the loss spectra behavior suggests that the optimal concentration of the compatibilizers in the considered blends is close to 5 wt %. © 2001 John Wiley & Sons, Inc. J Appl Polym Sci 82: 1423–1436, 2001

Key words: poly(ethylene terephtalate); polyethylene; compatibilization; recycling

INTRODUCTION

Poly(ethylene terephthalate) (PET) and high-density polyethylene (HDPE) are used extensively in packaging of consumer and industrial products. Recognizable streams of these plastics can be recovered provided that they are collected and separated into its neat components. The environmental policy of many countries encourage the recycling of plastics.[1] Three methods of recycling are of interest: mechanical recycling including blending technologies, incineration with energy recovery, and feedstock recycling (pyrolysis, hydrogenation, gasification, chemiolysis). Of these three methods, the mechanical recycling is a straightforward and relatively simple way of recycling. Industrial wastes are relatively easy to deal with because their contamination levels are low. However, municipal polymer waste requires much

Correspondence to: M. Pluta; e-mail: mpluta@bilbo.cbmm.lodz.pl.

Contract grant sponsor: European Commission Project INCO-Copernicus; Contract grant number: IC15CT960731.

Journal of Applied Polymer Science, Vol. 82, 1423–1436 (2001)

more careful segregation and purification programs. For successful PET recycling, the removal of poly(vinyl chloride) (PVC) contaminants is especially important. PVC, less thermally stable than PET, generates at processing temperatures acidic compounds,[2] which catalyze hydrolytic ester bonds cleavage of PET chains. This leads to the deterioration and discoloration of recycled polymers.

Recyclates of PET and HDPE (abbreviated in this paper as R-PET and R-PE, respectively) usually contain admixtures of other incompatible polymers. A complete separation of these is difficult and/or expensive. The presence of polymer admixtures leads frequently to poor performance of the recycled material. However, the properties of such recycled plastics may be restored by addition to the recyclate of some carefully selected compatibilizers.[4,5] The use of compatibilizers can also generate some net reduction of recycling costs, because the segregation of polymer waste may carried out in a less careful manner. The mechanical recycling combined with blending technology seems to be a very promising route for successful plastic recycling, and should be a subject of considerable attention.

We have undertaken the studies of recycling of unsegregated waste plastics within the frame of the INCO-Copernicus project No. IC15CT960731. Among others, the recyclates of segregated R-PET and R-PE were chosen for compatibilized blending.[5] These polymers are widely used, and constitute a very large portion of recyclable polymer waste. Because of their inherent mutual incompatibility and incompatibility with admixtures present in their recyclates, the blending process was designed with addition of various compatibilizers to improve processing characteristics and final properties of blends. Fourteen compatibilizers were selected initially from the range of commercially available copolymers and functionalized polymers.[6] It was found that the best results for blending of recycled PET and HDPE were obtained for random copolymer of ethylene with glycidyl methacrylate (EGMA) and for maleated block copolymer of styrene with ethylene/butylene (SEBS-*g*-MA) when compatibilization was performed in a corotating twin-screw extruder.[6] The blending process was optimized for concentration of the compatibilizers and processing conditions. It was found that for average concentration of 25 wt % of R-PE in R-PET an addition of 4 pph of EGMA gives the best tensile and impact properties, while for compatibilization with SEBS the optimum concentration was roughly 10 pph.[6]

The best results for the blends containing 75% of R-PE and 25 wt % of R-PET was obtained with the addition of 3 pph of EGMA or 5 pph of SEBS.[6] The properties of the optimized blends containing 75 wt % of R-PET and 25 wt % of R-PE and 4 pph of EGMA allowed for smooth extrusion of 0.5–1.0-mm thick and 1000-mm wide films on an industrial scale. It was possible to follow the extrusion with uniaxial film drawing with the draw ratio up to 4.[7]

The aim of this study was to determine the role of the compatibilization process on the phase structure and viscoelastic properties of R-PET/R-PE blends. The pellets of blends prepared for our earlier compatibilization studies were used in this work. We chose two series of samples with various concentration of compatibilizers to trace possible interactions between components. Morphological features and some physical properties of noncompatibilized and compatibilized blends were investigated and compared. The phase structure was characterized using SEM, light microscopy, DSC, and WAXS techniques. Viscoelastic properties were determined using DMTA.

EXPERIMENTAL

Materials

Segregated scraps of R-PET and R-PE were used as the blend components. Recycled PET, coming from postconsumer soft drink bottles, was purchased from Replastic Co., Italy (trade name "Rilat"). It has a melt-flow index, MFI of 25.3 g/10 min (2.16 kg at 265°C) and intrinsic viscosity (IV) $[\eta]$ = 0.757 dL/g, as measured with Ubbelohde viscometer at 25°C[8] (a mixture of phenol and 1,1,2,2-tetrachlorethane in 6 : 4 wt. ratio was used as a solvent). The detailed studies of the composition and properties are described elsewhere.[8] An analysis of impurities level[6] demonstrated that R-PET contained 0.204 wt % of remnants of labels with glue and 0.006 wt % of PVC. The level of PVC impurities was within acceptable limit. The R-PE, obtained also from Replastic Co., Italy (trade name "Rilae") has MFI of 0.8 g/10 min (2.16 kg at 265°C). In that recyclate 3.9 wt % of iPP and 1.5 wt % of LDPE admixtures were detected.[9] Two compatibilizers were chosen: copolymer of ethylene with glycidyl metacrylate (GMA, 6 wt %) as reactive sites (EGMA, Sumi-

Table I List of Blends Prepared

Blend Code	Blend Components			
	R-PET (%)	R-PE (%)	SEBS-*g*-MA (pph)	EGMA (pph)
75 : 25/0	75	25	0	0
25 : 75/0	25	75	0	0
75 : 25/2S	75	25	2	0
75 : 25/5S	75	25	5	0
75 : 25/10S	75	25	10	0
25 : 75/2S	25	75	2	0
25 : 75/5S	25	75	5	0
25 : 75/10S	25	75	10	0
75 : 25/5E	75	25	0	5
75 : 25/10E	75	25	0	10
25 : 75/3E	25	75	0	3
25 : 75/5E	25	75	0	5

Abbreviations S and E refer to compatibilizers SEBS-*g*-MA and EGMA, respectively.

tomo Chemical Co., Ltd) and styrene–ethylene/butylene–styrene triblock copolymer containing 1.7 wt % maleic anhydride groups attached to its rubber (EB) midblock (SEBS PAB-192; Shell Development Co., USA). M_w of the blocks are 7500–35,000–7500, respectively. The styrene blocks content is 30 wt %.

Preparation

All components were carefully dried in a vacuum oven prior to blending: R-PET at 170°C for 4 h, R-PE and EGMA at 105°C for 2 h, SEBS at 80°C for 2 h. To avoid moisture absorption the components were dry blended in desired proportion immediately after drying, and still hot fed to the corotating twin-screw extruder (Mapre DS 40, screw diameter 30 mm, L/D = 33). The speed of the screws was set to 500 rpm (giving the residence time 40 s). The die temperature was maintained at 270°C. Other experimental details of reactive compatibilization with EGMA and SEBS are described elsewhere.[6] The compatibilized blends R-PET/R-PE with a ratio of main components 75 : 25 and 25 : 75 were prepared. The amount of a compatibilizer in these blends varied from 2 to 10 wt %. Two reference noncompatibilized R-PET/R-PE blends of compositions 75 : 25 and 25 : 75 were also prepared. The exact compositions of formed blends are shown in Table I. The extrudates were cooled in water and pelletized immediately after blending. The pellets of blends were used for the preparation of 1 mm-thick sheets by compression molding at 265°C. The sheets were slowly cooled down to room temperature, and afterwards annealed at 90°C for 1 h to avoid the cold crystallization effect upon heating during subsequent DMTA and DSC experiments. Reference samples of the blend components were prepared according to the same procedures.

Measurements

Specimens for all investigations were cut out from the compression-molded sheets. The melting behavior of the components, and that of the binary blends and blends with the highest amount of compatibilizers, was characterized using a DuPont TA 2000 differential scanning calorimeter (DSC) with a heating rate of 20°C/min.

The morphology of the noncompatibilized and compatibilized blends was examined by means of polarized light microscopy (light microscope equipped with Linkam hot stage) and by scanning electron microscopy (SEM, JEOL T300). For light microscopy observations 2.5 μm-thick sections were cut out at ambient temperature using an ultramicrotome (TESLA BS 490A) equipped with a freshly prepared glass knife. The observation of sections were carried out at temperature of 150°C, i.e., above the melting point of R-PE component. This procedure allowed to distinguish crystalline R-PET component from already molten R-PE. The SEM observation were conducted on freeze-fractured surfaces coated with gold by ion sputtering.

Wide-angle X-ray scattering (WAXS) was used for the study of influence of compatibilization on crystalline structure of blend components. Samples of individual components were investigated along with blend samples. Measurements were performed in reflection geometry at ambient temperature by means of an automated computer-controlled X-ray diffractometer operating at 30-kV and 30-mA (CuK_α radiation, filtered by a Ni filter) within 2θ range from 15 to 35° with a step of 0.05°.

The dynamical mechanical properties of all blends and their components were measured using a DMTA apparatus in a dual cantilever bending mode (Dynamic Mechanical Thermal Analyzer Mk III, Rheometric Scientific Inc.). The storage modulus, E', and loss factor, tan δ, were measured at a constant frequency of 1 Hz as a function of temperature, varying within the range from −130° to 240°C for the R-PET-rich blends

and from −130 to 130°C for the R-PE-rich blends. The heating rate was 2°C/min.

RESULTS AND DISCUSSION

Phase Morphology

Light Microscopy

Figure 1(a)–(c) presents micrographs of thin sections of selected R-PET-rich blends: noncompatibilized of composition 75 : 25 and compatibilized with 10 wt % SEBS-*g*-MA and EGMA. The observed sections were heated to 150°C to melt the R-PE component. Therefore, bright regions of images correspond to the crystalline fraction of the R-PET component, while dispersed dark areas reflect molten inclusions of the R-PE component. In both binary and compatibilized blends the major R-PET component forms a continuous matrix. Polyethylene domains in the noncompatibilized blend show irregular shapes due to poor dispersion and the coalescence likely occurring on the sample molding followed by slow cooling. The dispersion of R-PE domains improves with addition of the compatibilizer. It can be noted that dispersion is substantially finer in blends compatibilized with EGMA than with SEBS-*g*-MA [cf. Fig. 1(b)–(c)]. This difference was anticipated because maleic anhydride groups of SEBS-*g*-MA can interact only with the hydroxyl groups of PET, while glicydyl methacrylic groups of EGMA can interact with both hydroxyl- and carboxyl-terminal groups of polyester.[10] The size of polyethylene domains in the R-PET/R-PE blend varies in the range of 10−40 μm, while in the R-PET/R-PE/SEBS-*g*-MA blend it is approximately 5–30 μm and in the R-PET/R-PE/EGMA blend it is well below 5 μm. Similar microscopical observations were performed for R-PE-rich blends. Images obtained for noncompatibilized R-PET/R-PE 25 : 75 blend and compatibilized blends are shown in Figure 1(d)–(f). In the case of the 25 : 75 blend the dispersion of the minor R-PET component is significantly better than the dispersion of R-PE in the 75 : 25 R-PET/R-PE blend [cf. Fig. 1(a) and (d)]. This results presumably from the lower viscosity of R-PET than of R-PE during blending. Polarized light micrographs for R-PE-rich blends with addition of a compatibilizer [Fig. 1(e) and (f)] show fine crystalline structure of the R-PET phase dispersed in the molten dark R-PE matrix. Because further interpretation of optical micrographs of these blends is not straightforward, their phase morphology is discussed below on the basis of SEM observations.

SEM Observations

SEM images of freeze-fractured surface of R-PET-rich blends: binary and compatibilized with 10 wt % SEBS-*g*-MA or EGMA are presented in Figure 2(a)–(c), respectively. In the binary 75 : 25 blend [Fig. 2(a)] R-PE inclusions of the size ranging from 2.5 to 30 μm dispersed in the R-PET matrix can be observed (sizes similar to those estimated from light microscopy). The smooth surface of inclusions evidences their poor adhesion to R-PET. Addition of SEBS-*g*-MA to the blend decreases the size of the R-PE inclusions. In blends containing 10 wt % of SEBS-*g*-MA [Fig. 2(b)] the size of inclusions is within the range of 1.5 to 16 μm. More profound changes of phase morphology were observed in blends compatibilized with EGMA. As evidenced in Figure 2(c) the sizes of R-PE inclusions reaches the level about 0.8 μm in the blends with the highest amount of EGMA [Fig. 2(c)]. The morphologies of surfaces indicate improved adhesion between R-PET and R-PE in compatibilized blends.

In the binary R-PE-rich blend inclusions of the R-PET component are from 0.4 to 3.5 μm [Fig. 3(a)]. They are noticeably smaller than those of the R-PE phase dispersed in binary R-PET-rich blend [Fig. 2(a)]. Also, here, a poor adhesion between R-PET and R-PE is observed. Compatibilization of the R-PE-rich blends leads to a further increase of the dispersion of R-PET inclusions. At the highest compatibilizer content the sizes varies from 0.2 to 2.0 μm in blends with SEBS-*g*-MA, while from 0.18 to 1.0 μm in blends with EGMA. The appearance of the fractured surfaces of R-PE-rich blends compatibilized with SEBS-*g*-MA [Fig. 3(b)] or with EGMA [Fig. 3(c)] demonstrates improved adhesion at interfaces. Both light microscopy and SEM observations led to conclusions that compatibilizers change more effectively minor phase sizes in R-PET-rich blends than in R-PE-rich blends.

DSC Studies

Figure 4(a) presents the DSC melting thermograms of binary and compatibilized blends as well as of single components, processed at the same conditions, including the extrusion step. The thermogram of the R-PET specimen shows the glass transition (T_g) at 79.8°C and the melting peak

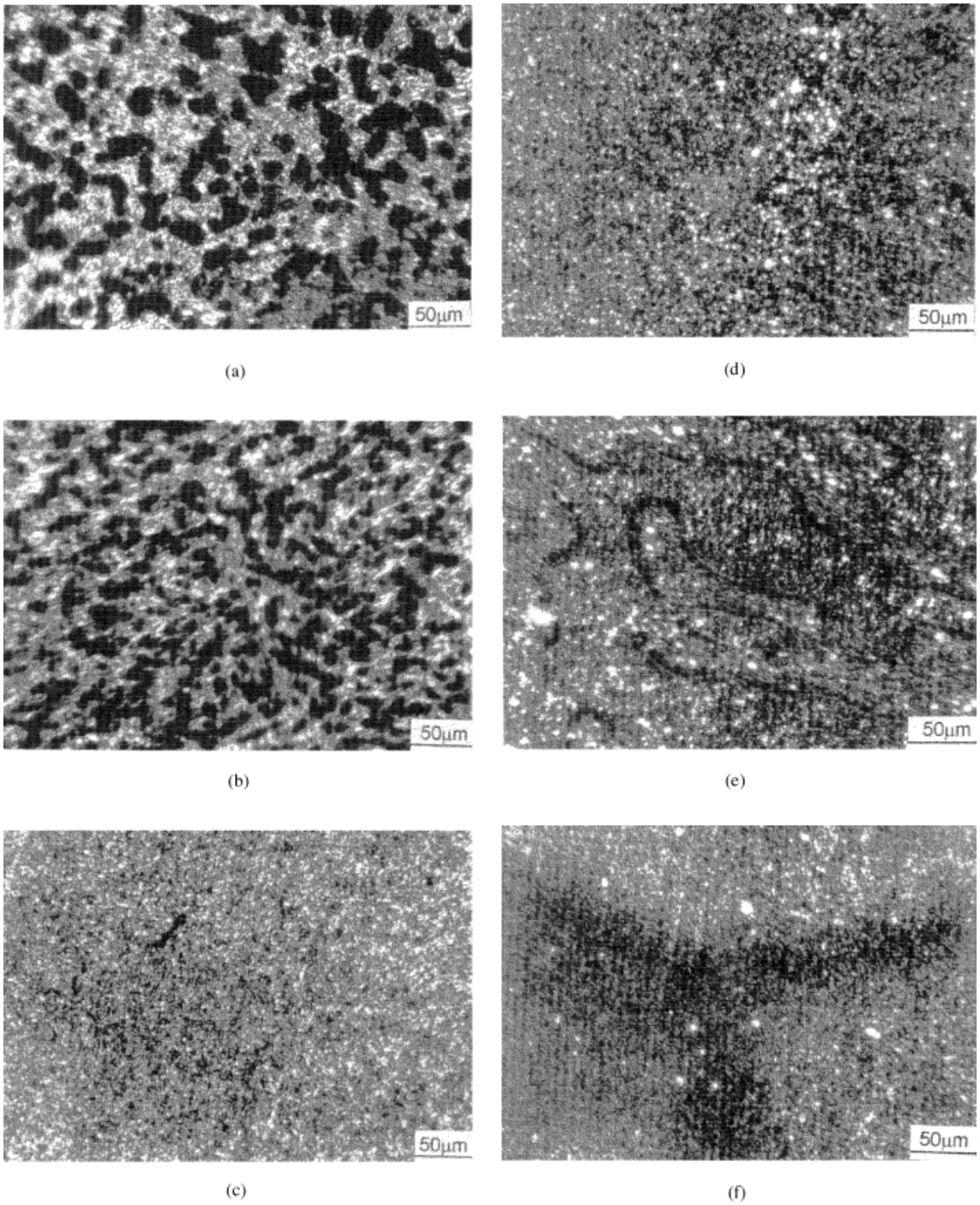

Figure 1 Polarized light micrographs of sections of R-PET-rich blends taken at 150°C: (a) R-PET/R-PE 75 : 25, (b) R-PET/R-PE/SEBS-*g*-MA 75 : 25/10, (c) R-PET/R-PE/EGMA 75 : 25/10, (d) R-PET/R-PE 25 : 75, (e) R-PET/R-PE/SEBS-*g*-MA 25 : 75/5, (f) R-PET/R-PE/EGMA 25 : 75/5.

(T_m) at 249°C. A cold crystallization peak is not observed due to high PET crystallinity of the samples. The DSC scan of R-PE specimen exhibits three transitions—the main melting peak at 132.9°C and two smaller contributions that originate from melting of LDPE and iPP admixtures. The T_g of R-PE was not observed due to relatively high crystallinity of this polymer. For specimen of

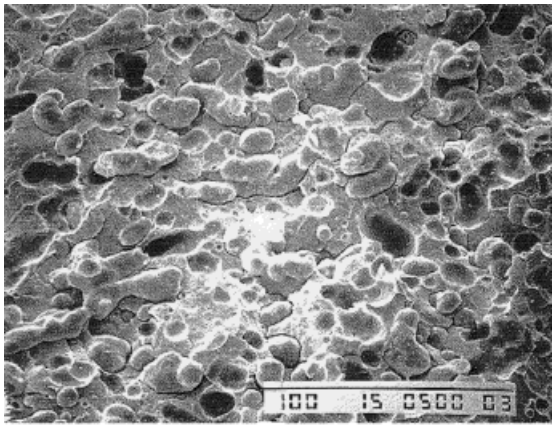

R-PET/R-PE 75:25

(a)

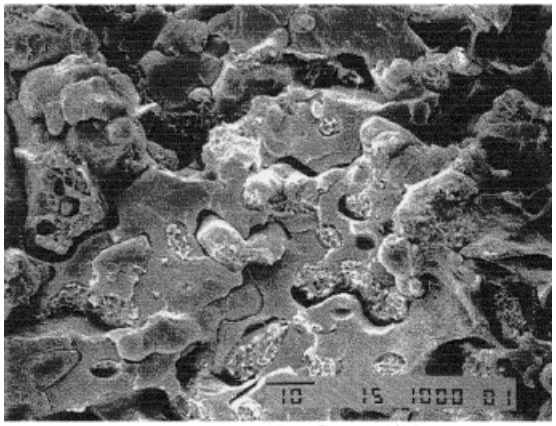

R-PET/R-PE/SEBS 75:25/10

(b)

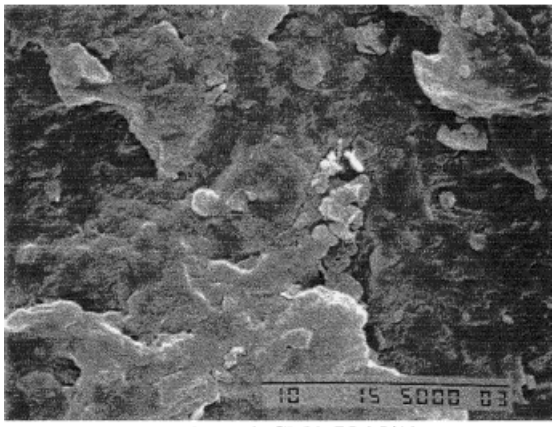

R-PET/R-PE/EGMA 75:25/10

(c)

Figure 2 SEM micrographs of fractured surfaces of R-PET-rich blends: (a) R-PET/R-PE 75 : 25, (b) R-PET/R-PE/SEBS-*g*-MA 75 : 25/10, (c) R-PET/R-PE/EGMA 75 : 25/10.

SEBS-*g*-MA the T_g detected at −49.4°C is followed by a broad and shallow endothermic effect in the range from −33 to 25°C. The thermogram of EGMA shows T_g at −8.6°C and melting peak at 121.4°C with onset of low temperature component at 30°C similar to R-PE. Thermograms of the binary R-PET-rich blend and those compatibilized with SEBS-*g*-MA show two endotherms representing melting of R-PET and R-PE components, while contributions from admixtures of LDPE and iPP are scarcely visible. In blends compatibilized with EGMA, in addition to the above-mentioned features, a melting process of EGMA can be recognized. Unfortunately, it coincides with melting of the less stable crystalline phase of R-PE; therefore, a separation of both contributions is difficult.

Figure 4(b) shows DSC melting thermograms of the R-PE-rich blends and plain components for reference. The R-PE component melting peak is larger and appears at slightly higher temperature than in the R-PET-rich blends. At the same time small melting effects of admixtures of LDPE and iPP can be recognized.

Calorimetric data determined from DSC scans are collected in Tables II and III. Degree of crystallinity of plain polymers (X_c) and the blend components [X_c(PET) and X_c(PE)] was calculated assuming the heat of fusion of the crystalline phase 119.8 J/g for R-PET[11] and 293 J/g for R-PE.[11] The T_m and X_c(PET) of the R-PET specimen was found to be 249°C and 43.4%, respectively. The temperature of the melting of the PET component in blends decreased slightly compared to plain R-PET. The crystallinity of the PET component in the blends also decreased compared to plain R-PET, yet more substantially than the temperature of melting. Moreover, crystallinity of the PET component in the R-PET-rich blends was depressed stronger than that in the R-PE-rich blends. The above changes demonstrate that the presence of polyethylene in the blends markedly influences the crystallization behavior of the PET component. On the other hand, the data presented in Tables II and III show that the crystallization of the PE component in the blends is much less influenced by the presence of other components than the crystallization of PET—only a small decrease of PE crystallinity was observed in the blends.

WAXS Measurements

X-ray measurements were performed as a complementary to the DSC studies to detect any dif-

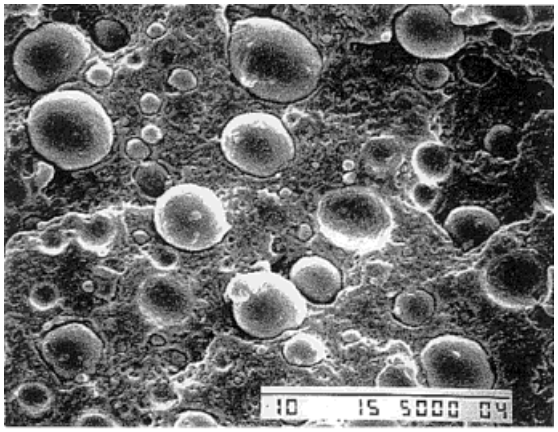

R-PET/R-PE 25:75

(a)

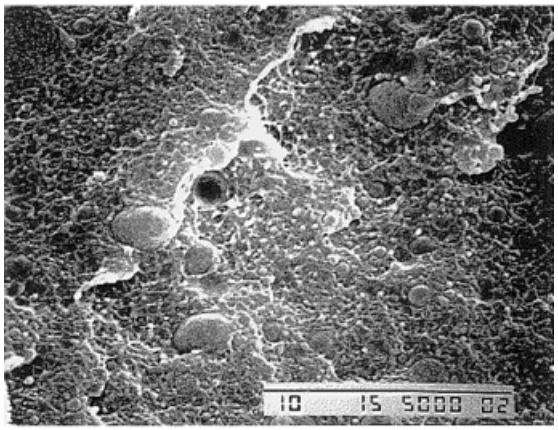

R-PET/R-PE/SEBS 25:75/10

(b)

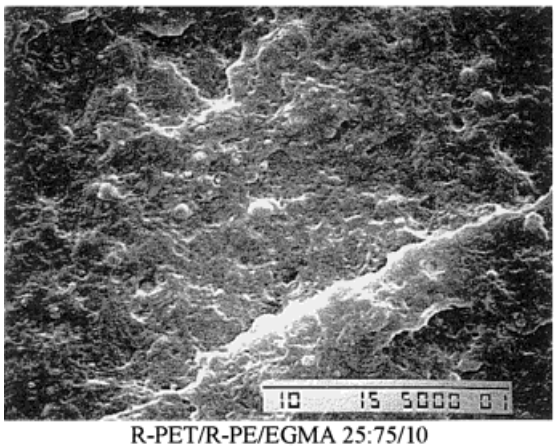

R-PET/R-PE/EGMA 25:75/10

(c)

Figure 3 SEM micrographs of fractured surfaces of R-PE-rich blends: (a) R-PET/R-PE 25 : 75, (b) R-PET/R-PE/SEBS-*g*-MA 25 : 75/10, (c) R-PET/R-HDPE/EGMA 25 : 75/5.

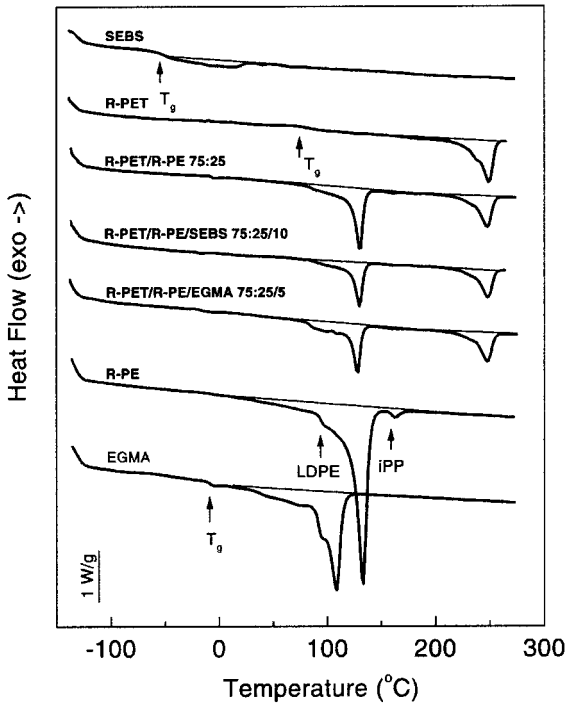

(a)

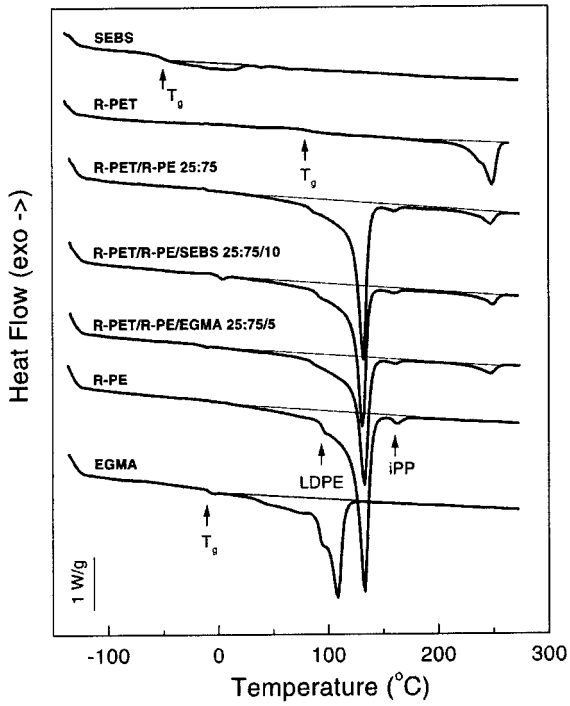

(b)

Figure 4 (a) DSC thermograms of R-PET-rich blends and components. The curves are normalized to the mass unit of the specimens. (b) DSC thermograms of R-PE-rich blends and components. The curves are normalized to the mass unit of the specimens.

Table II Calorimetric Characterization of Recyclates and Compatibilizers

Material	T_g (°C)	T_m (°C)	ΔH_m (J/g)	X_c (%)	PP Additive in R-PE	
					T_m (°C)	ΔH_m (J/g_{PE})
R-PET	79.8	249.0	52.0	43.4		
R-PE	—	132.9	196.2	69.9	162.5	5.15
SEBS	−49.4	12.0	10.0	3.4		
EGMA	−8.6	108.8	121.4	41.4		

In calculation of X_c the heat of fusion of crystalline PET phase equals 119.8 J/g, and the heat of fusion of crystalline PE phase equals 293.0 J/g was taken into account.[11]

ferences of the crystalline phase of PET and PE components in blends of different composition compared to plain components. The data collected from the DSC heating scan do not refer to the initial crystalline structure of the sample due to possible recrystallization phenomena occuring upon heating.

Figure 5(a) shows X-ray diffractograms recorded for binary and compatibilized R-PET-rich blends and for plain R-PET for reference, while Figure 5(b) presents diffractograms of R-PE-rich blends and reference R-PE. For the R-PET sample several diffraction maxima at the diffraction angles of 16.2°, 17.5°, 21.6°, 22.7°, 26.0°, and 32.5° can be observed. Similar maxima can be found in diffractograms of R-PET-rich blends along with sharper peaks near 21.6° and 23.9° produced by the crystalline phase of R-PE component. Diffractograms of the R-PE rich blends [Fig. 5(b)] reveal intense diffraction peaks at 21.6°, 23.9°, and a weak one at 30.0° associated with crystalline polyethylene, as well as small peaks at 16.9°, 27.3°, and 29.3°, resulting from diffraction on crystallites of iPP admixtures present in R-PE. Diffraction peaks of crystalline R-PET component are hardly visible due to much more intense contribution from diffraction on the major R-PE component.

The area under diffraction peaks corresponds to the degree of crystallinity of the respective component. The analysis of diffractograms confirms lower crystallinity of the R-PE component in binary blends compared to the reference R-PE sample. A stronger decrease was found in blends containing a compatibilizer. These estimations confirm DSC observations reported in the previous section. Unfortunately, low and diffuse PET diffraction peaks did not allowed for accurate estimation of the crystallinity of the PET component in blends. However, qualitative analysis of diffractograms seems to confirm a decrease of PET crystallinity found by DSC.

Viscoelastic Properties

Blend Components

The temperature dependencies of storage modulus, E', and mechanical loss, tan δ, of the recycla-

Table III Calorimetric Characterization of Binary and Compatibilized Blends of Recyclates

Blend Code	R-PE Component			R-PET Component		
	T_m (°C)	ΔH_m (PE) (J/g_{PE})	X_c (PE) (%)	T_m (°C)	ΔH_m (PET) (J/g_{PET})	X_c (PET) (%)
75 : 25/0	130.6	189.2	64.5	247.8	38.0	31.7
25 : 75/0	131.8	193.4	66.0	247.5	42.6	35.5
75 : 25/10S	131.2	171.2	58.4	248.3	37.7	31.4
25 : 75/10S	131.5	180.3	61.5	249.5	42.2	35.2
75 : 25/5E	128.1	185.2	63.2	247.9	37.2	30.8
25 : 75/5E	133.1	182.9	62.4	248.0	39.1	32.6

Abbreviations S and E refer to compatibilizers SEBS-*g*-MA and EGMA, respectively. In calculation of X_c the heat of fusion of crystalline PET phase equals 119.8 J/g, and the heat of fusion of crystalline PE phase equals 293.0 J/g was taken into account.[11]

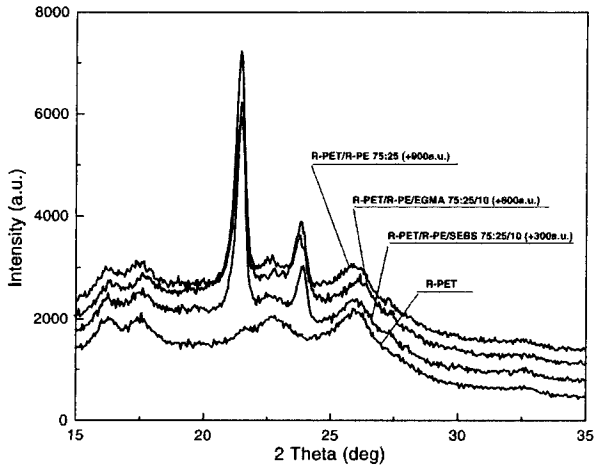

(a)

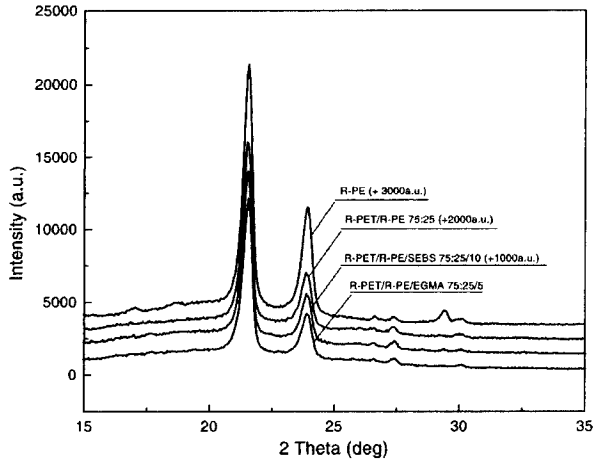

(b)

Figure 5 (a) WAXS 2θ distributions of R-PET-rich blends: (1) R-PET/R-PE 75 : 25, (2) R-PET/R-PE/SEBS-*g*-MA 75 : 25/10, (3) R-PET/R-PE/EGMA 75 : 25/10, and (4) R-PET sample. (b) WAXS 2θ distributions of R-PE-rich blens: (1) R-PET/R-PE 25 : 75, (2) R-PET/R-PE/SEBS-*g*-MA 25 : 75/10, (3) R-PET/R-PE/EGMA 25 : 75/5, and (4) R-PE sample.

tes and copolymers used for blend preparation are collected in Figure 6(a) and (b), respectively. The E' of R-PET gradually decreases with the temperature increase, and drops more rapidly above 75°C. This drop is accompanied by tan δ maximum ascribed to the main α relaxation process connected with the glass transition of PET.[12] This process is discernible even in samples in which glass transition of PET was difficult to detect by DSC. Secondary relaxation process, denoted as β, appears as a weak and broad maximum of tan δ with a peak near −65°C. It has been postulated[13] that the β process consists of two different components due to the motion of the carbonyl groups (low-temperature part) and phenyl ring flips (high-temperature part). Both the α- and β-relaxations have been attributed to the amorphous component.

R-PE samples exhibit two remarkable relaxation processes inherent for linear polyethylene. The γ relaxation process related to the glass transition[14] manifests itself by a small maximum of the tan δ accompanied by a weak jump of the E'

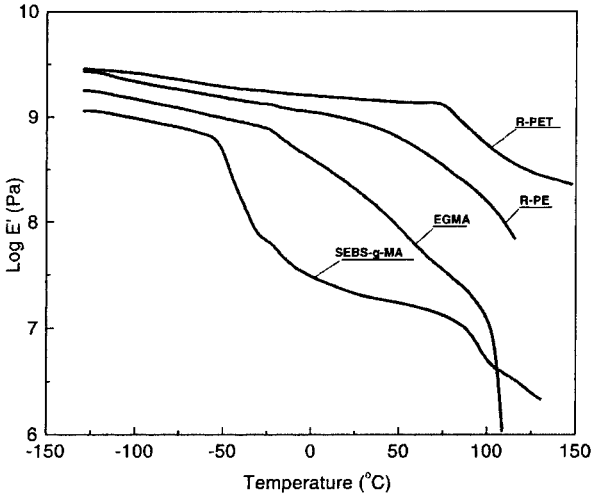

(a)

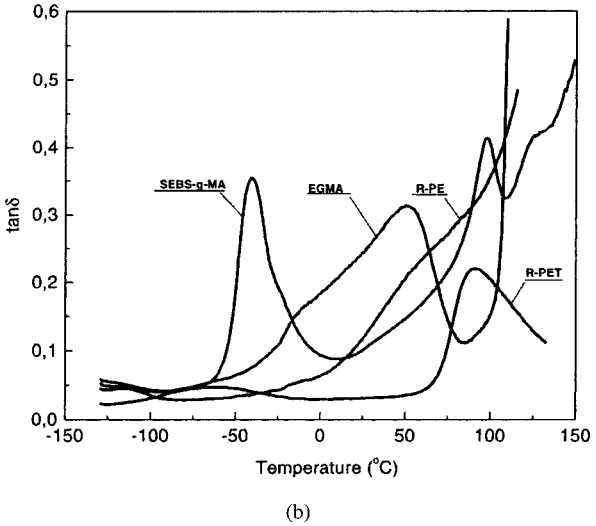

(b)

Figure 6 (a) Dynamic storage modulus (E') vs. temperature for R-PET, R-PE, SEBS-*g*-MA, and EGMA measured in the bending mode at 1 Hz. (b) The dependencies of mechanical loss vs. temperature for R-PET, R-PE, SEBS-*g*-MA, and EGMA measured in the bending mode at 1 Hz.

around −120°C. This transition was hardly detected on the DSC thermograms. Above 30°C, the tan δ increases due to activation of the mechanical α relaxation process related to the crystalline regions. At the same time modulus E' decreases distinctly with temperature. The α process is composed of two components, low-temperature, α_1 and high-temperature, α_2. It is believed that the α_1 process is focused on the grain-boundary phenomena (e.g., ref. 15), while the α_2 process is related to the molecular motion within crystallites (e.g., ref. 16). The β-relaxation process, clearly observed in branched polyethylene,[17] while nearly absent in linear polyethylene, is hard to detect on the tan δ curve of R-PE.

The temperature dependencies of the E' modulus of SEBS-*g*-MA exhibits two step drops: in subzero and positive temperature range. They are accompanied by distinct maxima on the tan δ curve appearing at −41°C and 98°C, respectively. Both relaxations are attributed to the glass transitions of ethylene/butylene and styrene blocks of the copolymer, respectively. Above the upper glass transition the mechanical loss of SEBS-*g*-MA increases due to premelting of the ethylene blocks of the copolymer.

For EGMA a drop in the E' coincides with sharp enhancement of the tan δ around −12°C. With further temperature rise tan δ develops a maximum around 50°C. The former effect is due to the glass transition; the latter one reflects intensification of mechanical loss related to crystalline regions.

R-PET-Rich Blends

To examine the influence of compatibilizing additives on the relaxation processes the amount of SEBS-*g*-MA and EGMA was varied from 0 to 10 wt %. The viscoelastic behavior of R-PET-rich blends compatibilized with SEBS-*g*-MA will be discussed first. The temperature dependencies of the E' and tan δ for these systems are presented in Figure 7(a) and (b), respectively. The temperature behavior of the E' is qualitatively similar to that for plain R-PET. The differences are observed in the values of E'. For blends, the values of E' are slightly lower than for plain R-PET and decrease continuously with increasing the amount of SEBS-*g*-MA in the blend. The tan δ spectra for the blends are quite complex, especially in the positive temperature range, where contributions from blend components overlap [compare Fig. 6(b) and Fig. 7(b)]. Therefore, a compatibilization effect can be analyzed only on the basis of changes of the tan δ maximum in the region of the β-relaxation of PET where contribution from the minor polyethylene phase is negligible. In Figure 7(b) a systematic increase of this maximum is clearly seen from approximately −63.0°C for plain R-PET to the temperatures of

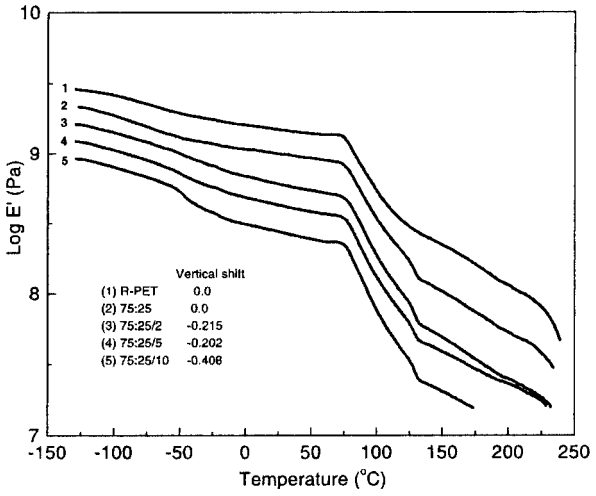

(a)

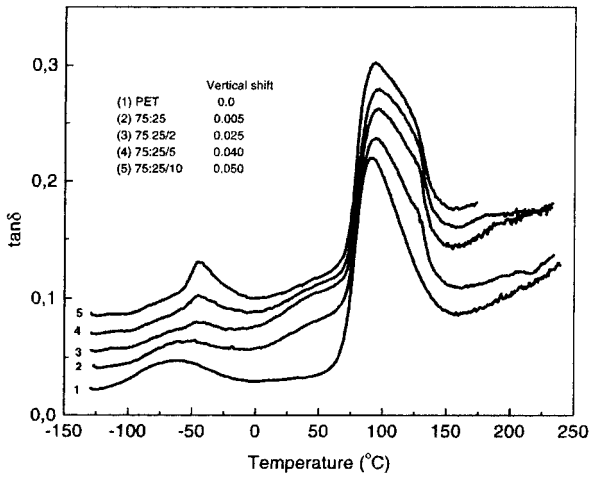

(b)

Figure 7 (a) Dynamic storage modulus (E') vs. temperature for R-PET-rich blends compatibilized with SEBS-*g*-MA and for the R-PET reference sample. Description of the curves and factor of their vertical shift are given in the insert. Measurements in the bending mode at 1 Hz. (b) The dependencies of tan δ vs. temperature for R-PET-rich blends compatibilized with SEBS-*g*-MA and for the R-PET reference sample. Description of the curves and factor of their vertical shift are given in the insert. Measurements in the bending mode at 1 Hz.

−60.0, −56.9, −45.6, and −44.8°C for R-PET/R-PE blends with an SEBS-*g*-MA content of 0, 2, 5, and 10 wt %, respectively (the maximum of relaxation of compatibilizer was found at −40.5°C). Moreover, above 2 wt % of SEBS-*g*-MA the high-temperature side of this maximum intensifies and eventually forms a small peak centered at the temperature close to that of plain compatibilizer. It may be guessed that this contribution is generated by a fraction of compatibilizer not involved at PET-PE interfaces, presumably separated from R-PET matrix in the form of separate inclusions. This hypothesis is plausible, because an increase of interface area caused by improved dispersion of the minor component leads to attenuation of the considered tan δ peak, as evidenced by mechanical loss spectra for R-PE-rich blends compatibilized with the same amount of SEBS-*g*-MA, presented in the following section.

A detailed analysis of the α(PET) relaxation process is more difficult because it is masked by significant contribution of the α(PE) relaxation, and additionally by an upper relaxation of the compatibilizer. For the binary R-PET-rich blend the contribution of the minor R-PE phase leads to broadening of the tan δ maximum in the α(PET) relaxation region. At the same time its position shifts towards a higher temperature and the high-temperature shoulder is enhanced. For ternary blends these effects become even more pronounced due to upper relaxation of the compatibilizer.

Viscoelastic data of R-PET-rich blends compatibilized with EGMA are presented in Figure 8(a) and (b). Similar to blends compatibilized with SEBS, the storage modulus of blends compatibilized with EGMA is lower than that of plain R-PET and uncompatibilized blend in the entire temperature range studied [see Fig. 8(a)]. Figure 8(b) shows that the position of maximum tan δ related to the β-relaxation of PET increases slightly from −63°C (plain R-PET) to −62.2, −61.5, and −60.1°C for blends containing 0, 5, and 10 wt % of EGMA, respectively, i.e., towards β-relaxation of EGMA (−12°C). In the range of α(PET) relaxation process the contributions of R-PE (α-relaxation of PE) and EGMA compatibilizer can be observed, similar to previously discussed blends compatibilized with SEBS-*g*-MA. The contribution from R-PE in the binary blend manifests as a shift of the tan δ maximum by approximately +4°C associated with the development of the high-temperature shoulder. For the ternary blends this shoulder is still present; however, the peak temperature of the resultant tan δ maximum decreases with an increase of the EGMA content. This is because the mechanical loss maximum of EGMA component precede those for the R-PET in the considered temperature range.

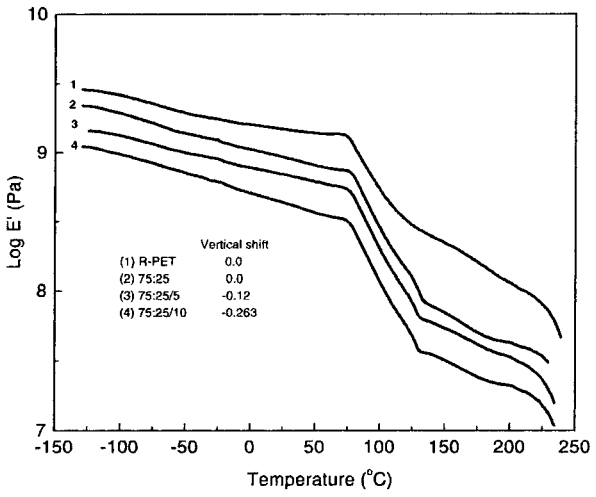

(a)

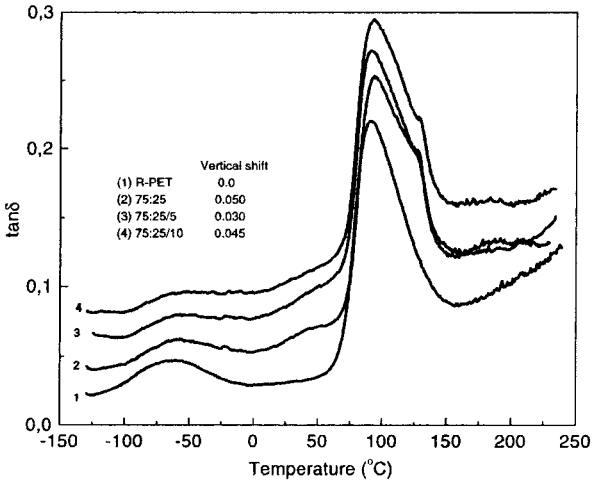

(b)

Figure 8 (a) Dynamic storage modulus (E') vs. temperature for the R-PET-rich blends compatibilized with EGMA and for the R-PET reference sample. Description of the curves and factor of their vertical shift are given in the insert. Measurements in the bending mode at 1 Hz. (b) The dependencies of tan δ vs. temperature for R-PET-rich blends compatibilized with EGMA and for the R-PET reference sample. Description of the curves and factor of their vertical shift are given in the insert. Measurements in the bending mode at 1 Hz.

R-PE-Rich Blends

Viscoelastic behavior of R-PE-rich blends compatibilized with SEBS-*g*-MA and EGMA is illus-

trated in Figure 9(a) and (b) and Figure 10(a) and (b), respectively. The modulus E' of binary and compatibilized blends is, as expected, within the limits created by moduli of plain components. Mechanical loss spectra for the blends compatibilized with SEBS-*g*-MA [Fig. 9(a)] and with EGMA [Fig. 10(a)] are dominated by the response of the major R-PE component. For this reason any possible

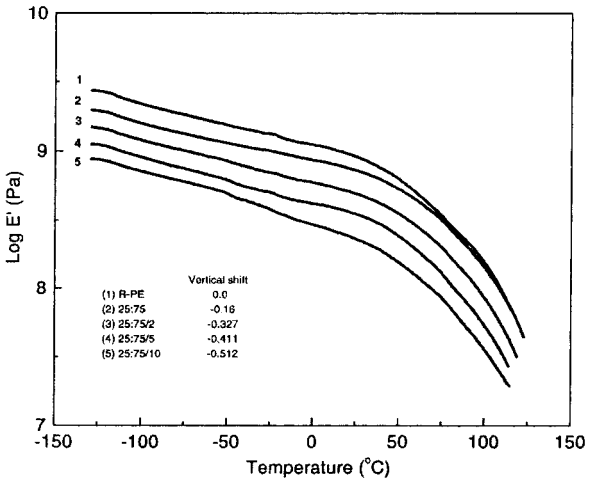

(a)

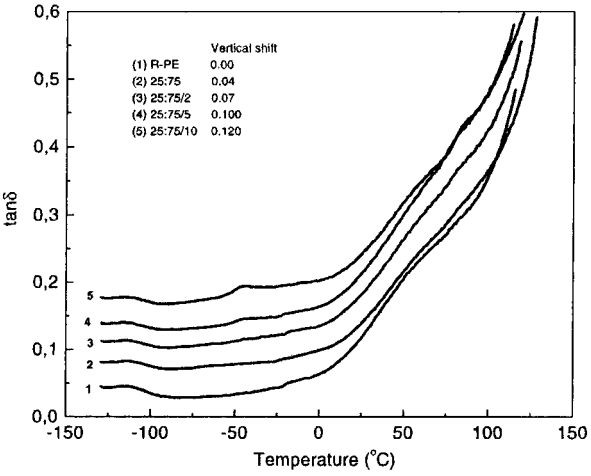

(b)

Figure 9 (a) Dynamic storage modulus (E') vs. temperature for R-PE-rich blends compatibilized with SEBS-*g*-MA and for the R-PE reference sample. Description of the curves and factor of their vertical shift are given in the insert. Measurements in the bending mode at 1 Hz. (b) The dependencies of tan δ vs. temperature for R-PE-rich blends compatibilized with SEBS-*g*-MA and for the R-PE reference sample. Description of the curves and factor of their vertical shift are given in the insert. Measurements in the bending mode at 1 Hz.

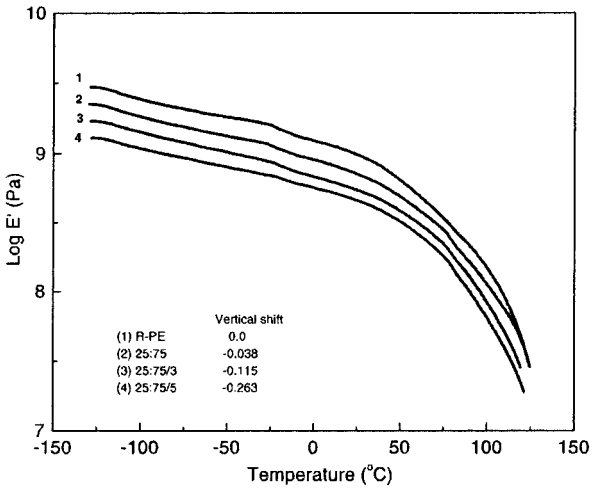

(a)

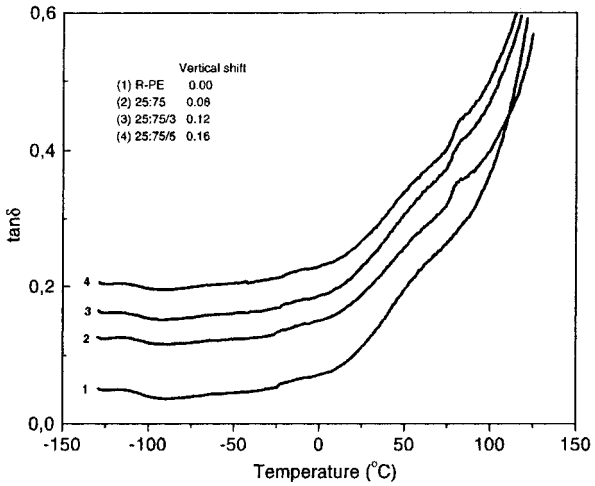

(b)

Figure 10 (a) Dynamic storage modulus (E') vs. temperature for R-PE-rich blends compatibilized with EGMA and for the R-PE reference sample. Description of the curves and factor of their vertical shift are given in the insert. Measurements in the bending mode at 1 Hz. (b) The dependencies of tan δ vs. temperature for R-PE-rich blends compatibilized with EGMA and for the R-PE reference sample. Description of the curves and factor of their vertical shift are given in the insert. Measurements in the bending mode at 1 Hz.

changes in the β(PET) relaxation process of the minor R-PET component are difficult to analyze. The contribution of minor components in the α(PE) relaxation region is also small. It manifests only as a weak fluctuation of the tan δ curve, in the region of T_g of PET, more pronounced in blends compatibilized with EGMA than those with SEBS-*g*-MA. Consequently, it is difficult to

evaluate any compatibilization phenomena on the basis of tan δ curves of R-PE-rich blends. Unfortunately, the changes in mechanical loss expressed by the loss modulus E'' (curves not presented here) are also obscured by overlapping contributions of the blend components, and do not provide any further information.

It is interesting to note that, contrary to the R-PET-rich blends, the R-PE-rich blends compatibilized with the same SEBS-*g*-MA amount (above 2 wt %) reveal on the tan δ curve only a small peak in the vicinity of −44°C ascribed to mechanical loss activated in the compatibilizer due to its low-temperature glass transition. This effect can be explained considering different interface area in both blends. The interface area is related to the dispersion of the minor component which, according to SEM observation, is finer in R-PE-rich blends than in R-PET-rich blends. Amount of the compatibilizer located within phase boundary regions, i.e., being effectively involved in compatibilization of the blend components, increases with an increase of the interfacial area. It may be expected that if the amount of compatibilizer in the blend is too large some fraction of it must be outside of PET-PE interface and form separate inclusions. Material in these inclusions should generate a peak of mechanical loss at the position close to that of plain component, as in the case of the R-PET-rich blend with a high level of SEBS-*g*-MA. Therefore, one can evaluate an optimum amount of SEBS-*g*-MA compatibilizer as below 5 wt % for the R-PET-rich blend and at 5 wt % for R-PE-rich blends. A similar conclusion can be drawn for the level of EGMA in the R-PET/R-PE blends. The results of optimization of concentration of EGMA in the R-PET/R-PE blends as well as processing conditions confirmed the above conclusion.[7]

CONCLUSIONS

The role of compatibilization on the phase structure and viscoelastic properties of blends of recyclates PET/PE was studied in this article. Two selected copolymers, SEBS-*g*-MA and EGMA, were examined in this studies as possible compatibilizers of recycled PET and PE. The main conclusions drawn in this study may be summarized as follows:

1. The recyclates of PET and PE from sorted household waste, and provided by commercial companies from Italy and Poland, contained 0.21 wt % and 5.4 wt % of admixtures, respectively, which were identified as other polyolefines. Such admixtures reduce performance of these recyclates, yet do not disqualify them for further processing.
2. Addition of the compatibilizer to the R-PET/R-PE blend changes remarkably the phase morphology of the blend, and greatly improves dispersion of the minor blend component. Compatibilization of both R-PET-rich and R-PE-rich blends with EGMA was more effective in relation to the size of dispersed phase than with SEBS-*g*-MA.
3. The DSC studies of the melting behavior revealed some changes in the temperature of melting and degree of crystallinity of the blend components. It was found that the presence of polyethylene in the blends markedly influences crystallization of the PET component. On the other hand, crystallization of the PE component in the blends is much less influenced by the presence of other blend components than the crystallization of PET. Addition of the compatibilizer does not substantially change the crystallization behavior of blends.
4. The DMTA data demonstrate a complex behavior of the loss spectra due to an overlap of the relaxation processes ascribed to the respective blend components. Consequently, any possible modifications of the main relaxation processes of R-PET and R-PE components are obscured by relaxations of other components. Interaction of the compatibilizer with R-PET component manifests in DMTA data through temperature shift and the intensity change of the β(PET) relaxation process. This effect is much more visible for the R-PET-rich blends compatibilized with SEBS-*g*-MA than those compatibilized with EGMA. In the case of R-PE-rich blends a similar trend was observed, only at the highest compatibilizer concentration. An analysis of the loss spectra behavior suggests the optimal concentration of the compatibilizers in the considered blends close to 5 wt %.
5. It is worth noting here that our other studies[6,7] have shown that the mechanical properties (tensile and impact) of R-PET-rich blends are markedly improved upon addition of EGMA, while for R-PE-rich blends better performances (elongation to break) are obtained using SEBS-*g*-MA.

The results obtained are interesting from a practical viewpoint because it indicates another effective way of restoring the properties of polymer recyclates.

This work was supported by European Commission project INCO-Copernicus, No. IC15CT960731.

REFERENCES

1. Blohm, H. P.; The, J. W.; Rudin, A. J Appl Polym Sci 1998, 70, 2081.
2. Milgrom, J. Plastic Recycling: Hanser Publishing: Munich, 1972, p. 45.
3. Kalfoglou, N. K.; Skafidas, D. S.; Kallitsis, J. K. Polymer 1995, 23, 4453.
4. Mantia, F. P. L. Macromol Symp 1998, 135, 157.
5. Pracella, M.; Galeski, A. Proc. First Italian-Jordanian Conference on Plastic Materials: Technology, Industry and Environment, Amman, Jordan, March, 1998.
6. Pracella, M.; Galeski, A.; Kummerloewe, C.; Lednicky, F. 6th European Symposium on Polymer Blends, Mainz, May, 1999.
7. Morawiec, J.; Krasnikowa, N. P.; Pracella, M.; Galeski, A. J Appl Polym Sci, to appear.
8. Pawlak, A.; Pluta, M.; Morawiec, J.; Galeski, A.; Pracella, M. Eur Polym J 2000, 36, 1875.
9. Report of INCO-COPERNICUS Project, Contract No. IC15 CT960731, 1999.
10. Kalfoglou, N. K.; Skafidas, D. S.; Kallitsis, J. K.; Lambert, J.-C.; Van der Stappen, L. Polymer 1995, 36, 4453.
11. Wunderlich, B.; Dole, M. J Polym Sci 1957, 24, 201.
12. McCrum, N. G.; Read, B. E.; Williams, G. In Anelastic and Dielectric Effects in Polymeric Solids; Wiley: New York, 1967, p. 353.
13. Maxwell, A. S.; Monnerie, L.; Ward, I. M. Polymer 1998, 39, 6851.
14. Takayanagi, M. Proceedings of the Fourth International Congress on Rheology; Interscience: New York, 1964.
15. Saito, N.; Okano, K.; Iwayanagi, S.; Hideshima, T. In Solid State Physics; Ehrenreich, H.; Seitz, F.; Turnbull, D. Eds.; Academic Press: New York, 1963, p. 458, Vol. 14.
16. Peterlin, A.; Fischer, E. W.; Reinhold, C. J Chem Phys 1962, 37, 1403.
17. Kline, D. E.; Sauer, J. A.; Woodward, A. E. J Polym Sci 1956, 22, 455.